



# Advanced Multi-Modeling of PWR Dynamics and Deep Learning based Computational Tool in SIMULINK and LabVIEW

Arshad H. Malik<sup>1\*</sup>, Aftab A. Memon<sup>2</sup>, and Feroza Arshad<sup>3</sup>

<sup>1</sup>Department of Maintenance Training, Pakistan Atomic Energy Commission, A-104, Block-B, Kazimablad, Model Colony, Karachi, Pakistan

<sup>2</sup>Department of Telecommunication Engineering, Mehran University of Engineering and Technology, Jamshoro, Sindh, Pakistan

<sup>3</sup>Department of Management Information System, Pakistan Atomic Energy Commission, B-63, Block-B, Kazimablad, Model Colony, Karachi, Pakistan

**Abstract:** The reactivity monitoring, prediction, and investigation is the most important parameter to ensure the safety and reliable operation of a nuclear power plant. This parameter is gained further importance in Pressurized Water Reactor (PWR) due to more sophisticated reactivity insertion mechanisms and innovative reactor core fuel loading scheme. Based on deterministic internal and external dynamics and neutronics analysis of Advanced PWR, all the reactivity feedback effects such as Doppler effect, moderator effect, control rod effect, liquid boron effect and reactor poisons effect are investigated, modeled and stochastically optimized using deep artificial intelligence. Advance Pressurized Water Reactor (APWR) of 600 MWe rating (AP-600) is used as a reference reactor model and based on the dynamics of AP-600, an Advanced Pressurized Water Reactor Dynamics and Intelligent Stochastic Optimization based Deterministic Neutronics Simulation (APD-ISO-DNS) Code is developed in the hybrid SIMULINK and LabVIEW environments. AP-600 reactor model is fine-tuned and adjusted for 300 MWe PWR (P-300) and 1070 MWe Advanced Chinese PWR (ACP-1000) using neutronics parameters and operational dynamic data of operating PWR nuclear power plants in Pakistan. Various load reduction transient experiments are conducted and dynamic transient simulations of P-300, AP-600 and ACP-1000 are evaluated in SIMULINK and in LabVIEW environments and found as per design basis.

**Keywords:** Multi-Model PWR Dynamics, Deterministic Reactor Neutronics, Deep Stochastic Optimization, Artificial Intelligence, Hybrid Simulation

## 1. INTRODUCTION

In this research work, a Pressurized Water Reactor (PWR) dynamics and neutronics are considered for state-of-the-art code development for P-300, AP-600 and ACP-1000.

A reactor dynamics model is developed based on the Point Reactor Kinetics Model (PRKM) with six precursor groups, internal reactivity feedbacks, and control rod reactivity [1]. The PRKM model with all internal and external reactivity feedbacks are models in [2]. This model is comprehensive and used for full fuel cycle modeling of nuclear reactor.

The PWR dynamics are further appended with decay heat for simulator development [3]. The practical aspects of 600 MWe PWR dynamics and neutronics for analyzer development for educational purposes are explored by micro simulation technology in [4]. A TRIGA research reactor and AP1000 PWR dynamics are evaluated for accident analysis in [5]. A TRIGA research reactor and VVER1000 PWR dynamics are evaluated for safety and transient accident analysis in [6]. The thermal hydraulics modeling of AP1000 PWR dynamics is carried out in RELAP code and compared with AP1000 using PCTAN in [7]. A data driven ANN based PHWR dynamics is modeled with moderator level

reactivity and control rod reactivity feedbacks in [8]. A fuzzy multi-model PWR dynamics is modeled for different power levels using control rod reactivity feedback in [9]. A research reactor PRKM neutronics is modeled and simulated with control rod reactivity feedback using LabVIEW in [10]. Further research is carried out in which web-based Graphical User Interface (GUI) is developed for PWR RELAP code in LabVIEW in [11]. A 3D neutron diffusion code for PWR fuel depletion and burn-up analysis is developed in [12]. A modelling approach using Deep Artificial Neural Network (DANN) optimized by a stochastic decent gradient algorithm is identified in [13]. Further research is carried out in [14, 15] in which deterministic data driven models are developed using PID based stochastic decent gradient optimizers. In [16], a hybrid simulation platform of MATLAB and LabVIEW is used to develop ANN models.

In this research work, a novel state-of-the-art hybrid simulation platform of Simulink and LabVIEW is used for designing, deterministic modeling, fine-tuning and Improved Stochastic Gradient Decent (ISGD) with Momentum (ISGD-M) based Optimization of Advanced Multi-PWR Dynamics and Neutronics of P-300, AP-600 and ACP-1000 for APD-ISO-DNS Code development. Therefore, this research work is one step ahead in the direction of advanced PWR dynamics and neutronics with most modern improved stochastic optimization used, for the first time, in nuclear industry. The proposed hybrid code is robust against parametric uncertainties and a highly accurate tool for advanced PWR dynamics and neutronics studies and nuclear reactor analysis, emphasising fuel cycle modelling of nuclear reactors.

## 2. MATERIALS AND METHODS

### 2.1 PWR Reactor Dynamics

There are hundreds of fission fragments in PWR, but 24 fission fragments or precursors are considered of comparable half-lives. Nuclear reactor kinetics is concerned with time dependent reactor power behavior caused by precursor concentration changes while the nuclear reactor dynamics is concerned with reactor power transients in which reactivity feedbacks caused by reactivity changes due to the

power change plays a vital role in over-all reactor behaviour.

### 2.2 Deterministic Modeling PWR Reactor Dynamics and Neutronics

The study of reactor kinetics and reactor dynamics is known as reactor neutronics.

In reactor core, reactor power is generated 93% by nuclear fission and 7% by decay heat, which can be modeled as [3]:

$$P(t) = P_{Fission}(t) + P_{Decay}(t) \quad (1)$$

Fission power is produced by fission fragments using multiple precursor groups. Fission power computed for six precursor groups is reported in [2], which is appended for 24 precursor groups in this research work as:

$$\frac{dP_{Fission}(t)}{dt} = \frac{\rho(t) - \beta}{\Lambda} P_{Fission}(t) + \sum_{m=1}^{24} \lambda_m C_m(t) \quad (2)$$

$$\frac{dC_m(t)}{dt} = \frac{\beta_m}{\Lambda} P_{Fission}(t) - \lambda_m C_m(t) \quad (3)$$

Where the symbols having their usual meanings.

Therefore, 25<sup>th</sup> order coupled reactor kinetics model is developed for short time scale modeling of nuclear reactor.

Decay heat is calculated using three decay product groups, which is calculated as [3]:

$$P_{Decay}(t) = \phi_T - \sum_{n=1}^3 (\gamma_n \phi_T - D_n(t)) \quad (4)$$

$$\frac{dD_n(t)}{dt} = \lambda_n (\gamma_n \phi_T - D_n(t)) \quad (5)$$

Where the symbols having their usual meanings.

The decay heat is used to calculate fuel and moderator temperatures. Therefore, 4<sup>th</sup> order coupled decay heat model is developed.

The heart of this research work is the sophisticated higher order coupled reactivity feedbacks model which is developed using all internal and external reactivity feedbacks taken into account.

The total reactivity is modeled as:

$$\rho(t) = \rho_{INTERNAL}(t) + \rho_{EXTERNAL}(t) \quad (6)$$

A very complex functional formulation of total internal reactivity as a function of internal reactivity feedbacks, initial reactor  $P_0$  and demanded reactor power  $P_D$ , Current reactor power and transient power (rate of change of power) such that  $\epsilon \{P_0, P_D\}$  is given by [2, 5]:

$$\rho_{INTERNAL}(t) = f \left( \begin{array}{c} \frac{dP(t)}{dt}, \frac{dT_F(t)}{dt}, \frac{dT_M(t)}{dt}, \\ \frac{d\rho_{Xe}(t)}{dt}, \frac{d\rho_{Sm}(t)}{dt}, P(t), P_0, P_D \end{array} \right) \quad (7)$$

Where the symbols having their usual meanings.

Similarly, the very complex functional formulation of total external reactivity as a function of external reactivity feedbacks is given by [2, 5]:

$$\rho_{EXTERNAL}(t) = g \left( \begin{array}{c} \frac{dP(t)}{dt}, \frac{d\rho_B(t)}{dt}, \frac{d\rho_{CR}(t)}{dt}, \\ P(t), P_0, P_D \end{array} \right) \quad (8)$$

Where the symbols having their usual meanings.

Therefore, overall, a higher order highly nonlinear dynamic model is developed for long time scale modeling of PWR reactor core.

### 2.3 Framework of APD-ISO-DNS Code

The Reactivity measurement and investigation is one of the challenges in PWR type nuclear power plants because the reactivity of the nuclear power reactor is not measured directly in PWRs. It is computed with dedicated nuclear reactor codes. Therefore, this research aims to design and develop an innovative computational tool for virtual total reactivity and reactivity feedback.

The analytical deterministic computational model developed for PWR transient dynamics is fine-tuned and simulated for P-300, AP-600 and ACP-1000 PWR-based nuclear power plants using plant operational data and reactor design data. Therefore, P-300, AP-600 and ACP-1000 reactor cores have higher order deterministic different

neutronics models.

The developed transient nuclear reactor model APD-ISO-DNS Code has three modules APD-ISO-DNS-300, APD-ISO-DNS-600 and APD-ISO-DNS-1000 for P-300, AP-600 and ACP-1000 PWR respectively as shown in Fig.1.

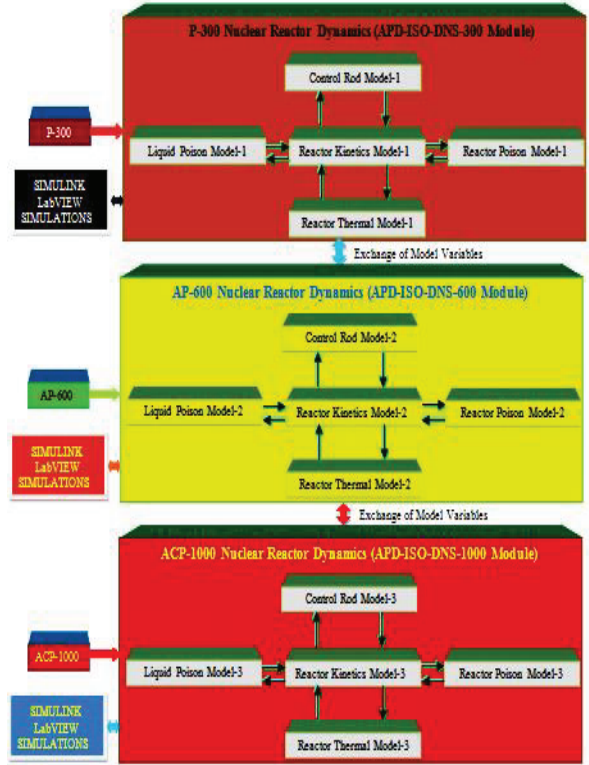


Fig. 1. Overall design of APD-ISO-DNS code.

Each module comprises four models known as reactor kinetics model, reactor poison model, liquid poison model, and control rod model. Reactor kinetics model is further composed of fission fragments dynamics and decay product dynamics. Reactor poison model is composed of Xenon and Samarium dynamics. Liquid poison model is composed of boron dynamics with different fuel conditions such as burn-up of fuel and different conditions of reactor core like Beginning of Core (BOC), Middle of Core (MOC) and End of Core (EOC) as shown in Fig. 2. Control rod model is composed of different control banks and overlapping logics.

The innovative reactor dynamics data is generated from the developed fine-tuned transient reactor dynamics models for APD-ISO-DNS-300, APD-ISO-DNS-600 and APD-ISO-DNS-1000

modules. These modules are used to design and develop an intelligent reactor dynamics code, now designated as APD-ISO-DNS Code. This code has an excellent reverse engineering capability to produce reactor power from reactivity feedback. After fine tuning, the APD-ISO-DNS code is modified to produce reactivity feedback and total reactivity directly from measured data of P-300, AP-600 and ACP-1000. The PWR neutronics tool is deterministic in nature which is optimized by stochastic technology.

## 2.4 Deep Artificial Intelligence

### 2.4.1 Concept of Deep Learning

Deep Artificial Neural Network (DANN) is an excellent intelligent tool for nonlinear pattern mapping or dataset. The term deep is used in the sense of dense or depth or more number of hidden layers with number of nodes in each hidden layer in an artificial neural network having multi-step processing. A neural network with more than three layers including input and output layer is considered for deep learning process. Deep learning is basically unsupervised learning capable to produce a highly accurate model.

### 2.4.2 Selection of Optimization Algorithm

Improved Stochastic Gradient Decent Momentum (ISGD-M) optimization based DANN is selected in this research work, which converges quickly and accurately. So, it is an Intelligent Stochastic Optimization (ISO) method for DANN. SGD is simply a Proportional Controller with gain  $K_p$ . SGD plus Momentum term (SGD-M) is a Proportional plus Integral Controller with gains  $K_p$  and  $K_i$ . There is a problem of overshoot associated with SGD-M optimizer, which is resolved by introducing a future prediction feature through Derivative Controller with gain  $K_D$ .  $K_D$  is called hyper-parameter. Now, SDM-M with hyper-parameter is designated as ISGD-M. Therefore, a PID controller based optimization is adopted for deep ANN training known as PID optimizer for DANN, which uses past, present and change of gradient for updating DANN weights [14].

In this DANN, input is mapped with output through a parameter  $\theta$ .  $\theta(t)$  is the weight of PID

optimizer. DANN is a three-layer deep ANN with two hidden layers in this research work. If  $W_{ji}$ ,  $W_{kj}$  and  $W_{lk}$  are layer weights between input layer and first hidden layer, first hidden layer and second hidden layer and second hidden layer and output layer respectively, then  $\theta = \{ W_{ji}, W_{kj}, W_{lk} \}$ , where  $i, j, k$  and  $l$  are the number of nodes or neurons in input, first hidden, second hidden and output layers respectively [15].

The difference between the desired actual reactivity feedback as an output parameter and deep ANN output as an predicted reactivity feedback is computed through loss function or error function  $L$ .  $\partial L / \partial \theta$  is called gradient. In fact, in this research work,  $\partial L / \partial \theta$  is  $\partial L(\theta, P(t), \dot{P}(t)) / \partial \theta$  because  $P(t)$  and  $\dot{P}(t)$  are inputs for all reactivity feedbacks. The gradient in deep ANN is basically having the similar concept as the error  $e(t)$  in PID controller.

The gradient between input layer and first hidden layer is given by:

$$e_{ji}(t) = \partial L(\theta(W_{ji}, W_{kj}, W_{lk}), (P(t), \dot{P}(t))) / \partial \theta(W_{ji})$$

The gradient between first hidden layer and second hidden is given by:

$$e_{kj}(t) = \partial L(\theta(W_{ji}, W_{kj}, W_{lk}), (P(t), \dot{P}(t))) / \partial \theta(W_{kj})$$

The gradient between second hidden layer and output hidden is given by:

$$e_{lk}(t) = \partial L(\theta(W_{ji}, W_{kj}, W_{lk}), (P(t), \dot{P}(t))) / \partial \theta(W_{lk})$$

The gradient in deep ANN works on the principle of moving average of gradients. The concept of feedback in PID controller is basically the back propagation in deep ANN. Therefore, as long as the gradient exists, weight is updated.

Learning rate ( $r$ ) is the most important parameter for deep ANN in this optimisation process. The optimal values of PID controller for DANN are  $K_p = 2r$ ,  $K_i = K_D = r$  [15]. There is one more important design parameter  $\alpha$ , which is known as balancing factor. This balancing factor is defined between past and current gradients. The derivative gain ( $K_D$ ) of PID is the most dominant parameter for stochastic optimization process.

The ideal value of hyper-parameter  $K_D$  is computed as [15]:

$$K_D = 0.5 + 0.25r + \left(1 + \frac{16}{9}\pi^2\right) / r \quad (9)$$

## 2.5 Intelligent Modeling of PWR Dynamics and Neutronics

### 2.5.1 Choice of Design Matrices, Vectors and Activation Functions for Sub DANN

Now, intelligent modeling of PWR neutronics is accomplished with DANN using stochastic optimization technique. Suppose  $H_{ji}$  and  $H_{kj}$  are the weight matrices of first and second hidden layers comprised of  $W_{ji}$  and  $W_{kj}$  weights respectively. In that case,  $M_{lk}$  is the weight matrix of output layer comprised of  $W_{lk}$  weights.  $B_j$ ,  $B_k$  and  $B_l$  are bias vectors of first hidden, second and output layers respectively then  $\Psi_j(\cdot)$ ,  $\Psi_k(\cdot)$  and  $\Psi_l(\cdot)$  are nonlinear activation functions, linear activation function of first hidden layer, second hidden layer and output layer respectively.

### 2.5.2 Modeling of Sub DANN for Reactivity Feedbacks

Now, all reactivity feedbacks for six sub ISO-DANN are modeled as:

$$\rho_F(t) = \Psi_l^F [M_{lk}^F \Psi_k^F \{H_{kj}^F \Psi_j^F (H_{ji}^F (P(t), \dot{P}(t)) + B_j^F) + B_k^F\} + B_l^F] \quad (10)$$

$$\rho_M(t) = \Psi_l^M [M_{lk}^M \Psi_k^M \{H_{kj}^M \Psi_j^M (H_{ji}^M (P(t), \dot{P}(t)) + B_j^M) + B_k^M\} + B_l^M] \quad (11)$$

$$\rho_{Xe}(t) = \Psi_l^{Xe} [M_{lk}^{Xe} \Psi_k^{Xe} \{H_{kj}^{Xe} \Psi_j^{Xe} (H_{ji}^{Xe} (P(t), \dot{P}(t)) + B_j^{Xe}) + B_k^{Xe}\} + B_l^{Xe}] \quad (12)$$

$$\rho_{Sm}(t) = \Psi_l^{Sm} [M_{lk}^{Sm} \Psi_k^{Sm} \{H_{kj}^{Sm} \Psi_j^{Sm} (H_{ji}^{Sm} (P(t), \dot{P}(t)) + B_j^{Sm}) + B_k^{Sm}\} + B_l^{Sm}] \quad (13)$$

$$\rho_{CR}(t) = \Psi_l^{CR} [M_{lk}^{CR} \Psi_k^{CR} \{H_{kj}^{CR} \Psi_j^{CR} (H_{ji}^{CR} (P(t), \dot{P}(t)) + B_j^{CR}) + B_k^{CR}\} + B_l^{CR}] \quad (14)$$

$$\rho_B(t) = \Psi_l^B [M_{lk}^B \Psi_k^B \{H_{kj}^B \Psi_j^B (H_{ji}^B (P(t), \dot{P}(t)) + B_j^B) + B_k^B\} + B_l^B] \quad (15)$$

## 3. RESULTS AND DISCUSSION

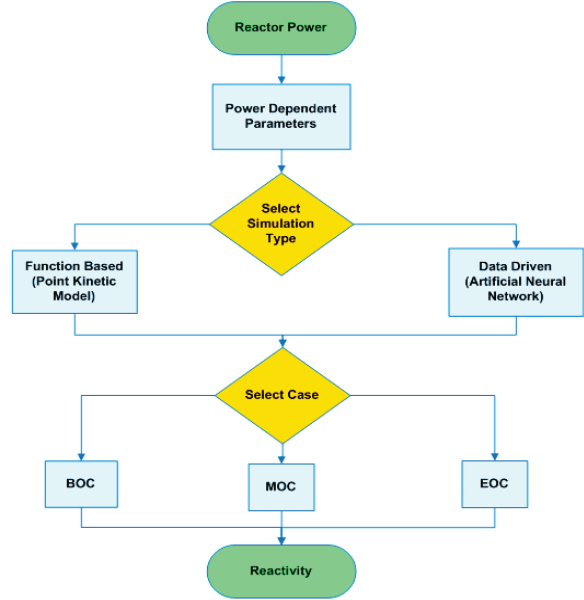


Fig. 2. Selection scheme for fuel burn-up along the fuel cycle length in APD-ISO-DNS code.

PCTTRAN is obtained from micro-simulation technology and is a product of International Atomic Energy Agency (IAEA). The process of obtaining the power dependent reactivity components or reactivity feedbacks using artificial intelligence is shown in Fig. 3.

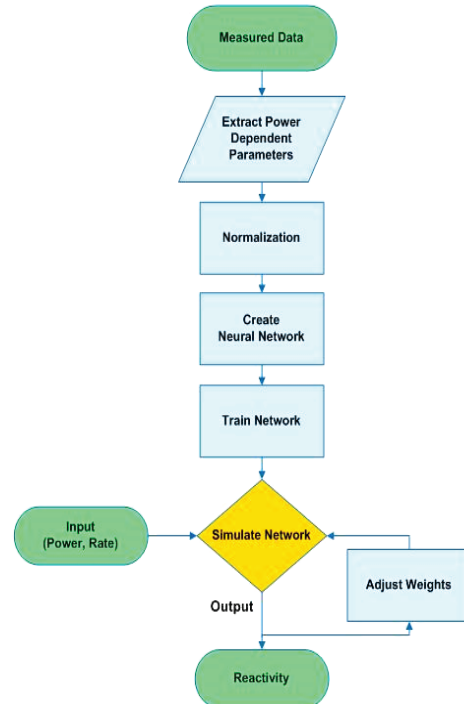


Fig. 3. Structure of intelligent data flow in APD-ISO-DNS code.

Therefore, the APD-ISO-DNS-600 module is best tuned and adjusted and used as a reference module or model for APD-ISO-DNS-300 and APD-ISO-DNS-1000 modules. APD-ISO-DNS-300 and APD-ISO-DNS-1000 modules are fine-tuned and adjusted using operational and design data of P-300 and ACP-1000. APD-ISO-DNS code is developed in hybrid Simulink and LabVIEW environments.

### 3.1 Evaluation of APD-ISO-DNS Code in SIMULINK

In this research work, APD-ISO-DNS code is developed for the first time for nuclear industry using ISGD-M optimized DANN in Simulink environment. There are six DANN designed for each reactivity feedback. The processing of data flow in all six Sub ISO-DANN is in parallel distributed fashion. The coupling scheme of all six Sub ISO-DANN in APD-ISO-DNS code is shown in Fig. 4.

The APD-ISO-DNS code is designed and developed using equations (10) through (16) optimized by hyper-parameter defined in equation (9). The Simulink model transient dynamics framework of APD-ISO-DNS code is shown in Fig. 5.

Eighteen design parameters of APD-ISO-DNS code are computed and optimized for P-300, AP-600 and ACP-1000. The detailed design parameters for moderator reactivity are tabulated in Table 1 for reference purposes. The optimized hyper-parameters for the entire six sub ISO-DANN for P-300, AP-600 and ACP-1000 are tabulated in Table 2.

In this research work, APD-ISO-DNS-600 module is evaluated for a load reduction transient in which reactor power is reduced from 100% to 60% in a sequence of 4 steps with a 10% step size using control rods as external reactivity mechanism because AP-600 is a base load nuclear power plant and its reactivity control is designed for 10% step change. Each step is executed at a rate of 2.31%/min embedded in the transient design. Practically, all step changes are designed with embedded ramp transients in AP-600. Since the reactor is 600 MWe PWR with medium scale nuclear power plant category, so ramp rate is 2.31%/min adopted in this transient. The innovative transient data which is specially generated using analytical model data, plant operational data and design data is now designated as “Experimental Data”. The training of fuel reactivity, moderator reactivity and control rod reactivity are shown in Fig. 6, Fig.7 and Fig. 8 respectively.

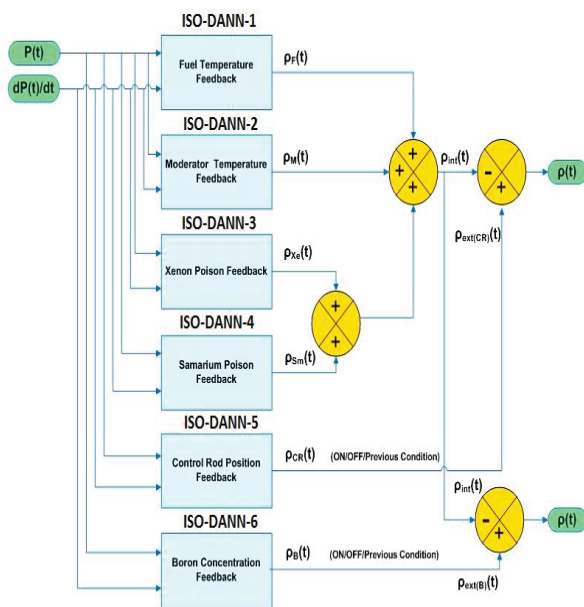


Fig. 4. Coupling of intelligent dynamic feedback design of APD-ISO-DNS code.

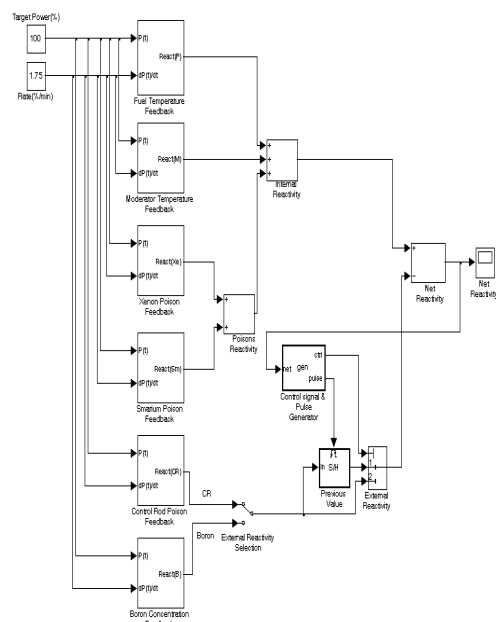


Fig. 5. Simulink model of APD-ISO-DNS code

**Table 1.** Parameters of APD-ISO-DNS-300 code for moderator reactivity

Reactor Type	Hyper-parameters of Different Variables	Design Values
P-300	Fuel Reactivity	10
P-300	Moderator Reactivity	12
P-300	Xenon Reactivity	18
P-300	Samarium Reactivity	16
P-300	Control Rod Reactivity	15
P-300	Boron Reactivity	11
AP-600	Fuel Reactivity	10
AP-600	Moderator Reactivity	12
AP-600	Xenon Reactivity	17
AP-600	Samarium Reactivity	15
AP-600	Control Rod Reactivity	14
AP-600	Boron Reactivity	11
ACP-1000	Fuel Reactivity	17
ACP-1000	Moderator Reactivity	13
ACP-1000	Xenon Reactivity	16
ACP-1000	Samarium Reactivity	15
ACP-1000	Control Rod Reactivity	29
ACP-1000	Boron Reactivity	22

**Table 2.** Optimized Hyper-parameter of APD-ISO-DNS

Intelligent Code Design Parameters	Design Values
Number of Nodes of Input Layer ( $i$ )	2
Number of Nodes of First Hidden Layer ( $j$ )	177
Number of Nodes of Second Hidden Layer ( $k$ )	177
Number of Nodes of Output Layer ( $l$ )	1
Number of training patterns (N)	25000
Number of Epochs	600
Balancing factor ( $\alpha$ )	1
Initial Learning Rate ( $r$ )	0.15
Optimal Hyper-parameter ( $K_D$ )	12
Final Learning Rate ( $r$ )	1.68
Performance gradient	0.001
Standard deviation	0.0005

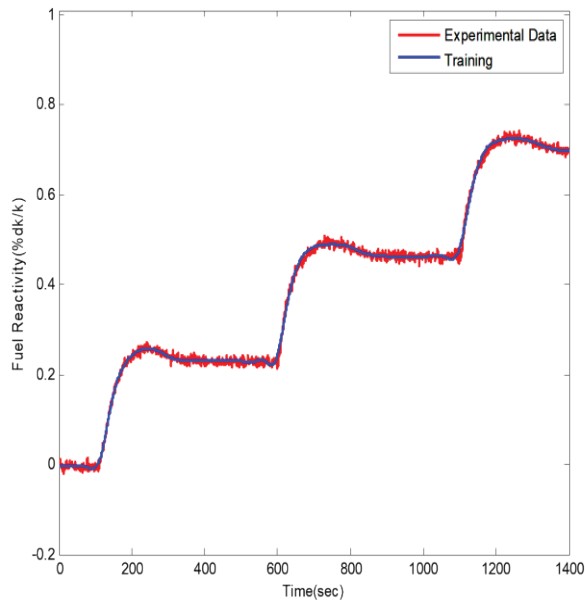


**Fig. 6.** Fuel reactivity of P-600 during learning phase of APD-ISO-DNS code.

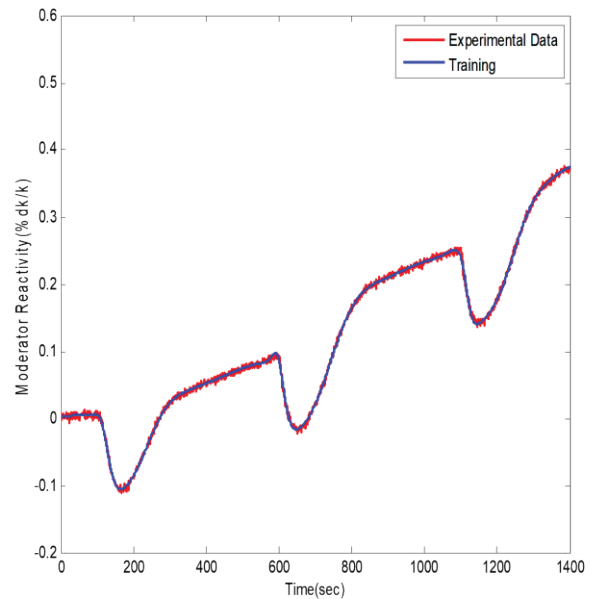


**Fig. 7.** Moderator reactivity of P-600 during learning phase of APD-ISO-DNS code.

There are six data sets for reactivity parameters. Therefore, in fact, there are six trends for training phase and six trends for validation phase. But due to space limitation and scope of this research work, three trends are shown for validation purposes. In validation phase, the pattern of error between predicted and experimental output is also realized. The fuel reactivity, moderator reactivity, control rod reactivity and total reactivity for validation phase are shown in Fig. 9, Fig.10, Fig. 11 and Fig. 12 respectively.

In this case study, it is observed that as the reactor power is reduced in steps, fuel reactivity and moderator reactivity increases as shown in Fig. 9 and Fig.10. This is because the fuel and moderator reactivity coefficients are negative.

Since the fuel and moderator reactivities are increased against reactor power reduction in steps, therefore, to cater this increase in total internal reactivity, control rod reactivity is decreased which in turn decreases the total external reactivity as shown in Fig. 11.

The validation is proved successfully because the total reactivity moves around zero that completely and safe ensures reactor criticality throughout the load reduction transient as shown in Fig. 12.

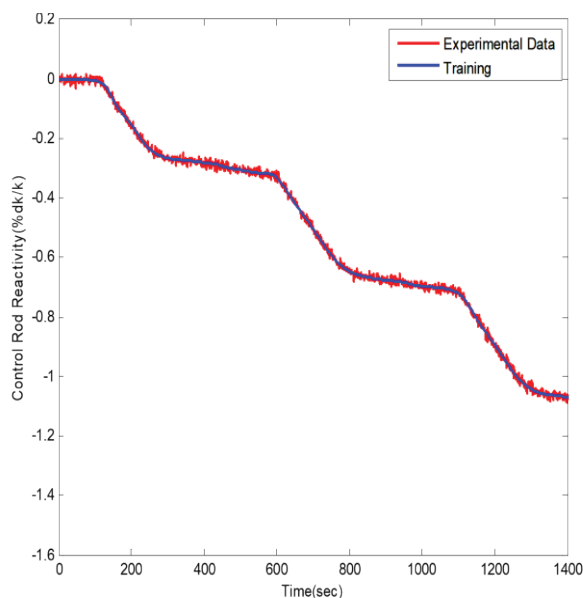


**Fig. 8.** Control rod reactivity of P-600 during learning phase of APD-ISO-DNS code.

All the results of APD-ISO-DNS-600 are as per specifications and reactivity bounds as laid down in [4].

Later, APD-ISO-DNS-300 module is evaluated for a load reduction transient in which reactor power is reduced from 100% to 75% at a rate of 5%/min because P-300 is a base load nuclear power plant of small scale category and its reactivity control is designed for maximum upto 5%/min embedded ramp rate. All the reactivity feedbacks are shown collectively in Fig. 13.

The variations of reactivity feedbacks are exactly similar to those in APD-ISO-DNS-600 module. All the results of APD-ISO-DNS-300 are as per specifications and reactivity bounds as laid down in Final Safety Analysis Report of P-300 which is standard report from the designer as a benchmark.

### 3.2 Evaluation of APD-ISO-DNS Code in LabVIEW

Now, in this research work, APD-ISO-DNS code is developed again for the first time in nuclear industry using ISGD-M optimized DANN in LabVIEW environment. PID optimizer based intelligent DANN VIs are designed and developed in LabVIEW for APD-ISO-DNS LabVIEW code as

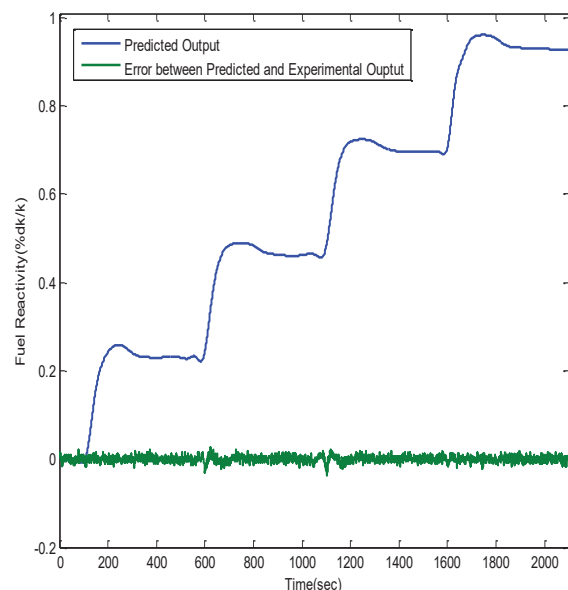


**Fig. 9.** Fuel reactivity of P-600 during validation phase of APD-ISO-DNS code.

shown in Fig. 14.

The LabVIEW block diagram code is developed for APD-ISO-DNS code that integrates transient dynamic Simulink model of APD-ISO-DNS code as shown in Fig. 15.

APD-ISO-DNS-1000 module is evaluated for a load reduction transient in which reactor power is reduced from 100% to 20% in a sequence of 4 steps with a 20% step size using control rods as external reactivity mechanism for the compensation of total internal reactivity because it is load following nuclear power plant of large scale category. In this

transient, each after 20% change in reactor power, it is held constant for 9 hours. Each step is executed at a 0.166%/min rate embedded in the transient design. A front panel is shown in Fig. 16, in which all the reactivity feedbacks are shown. The variations of reactivity feedbacks are exactly similar to those in APD-ISO-DNS-600 module.

All the results of APD-ISO-DNS-1000 are as per specifications and reactivity bounds as laid down in Final Safety Analysis Report (FSAR) of ACP-1000 which is standard report from designer as a benchmark.

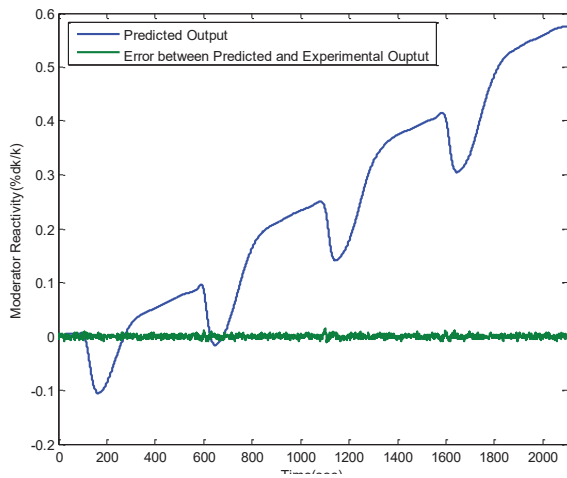


Fig. 10. Moderator reactivity of P-600 during validation phase of APD-ISO-DNS code.

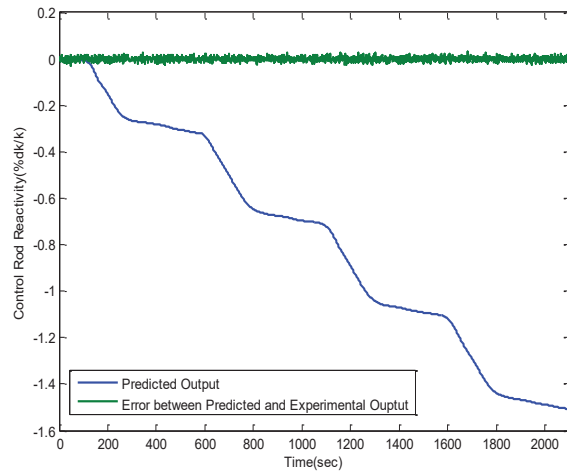


Fig. 11. Control reactivity of P-600 during validation phase of APD-ISO-DNS code.

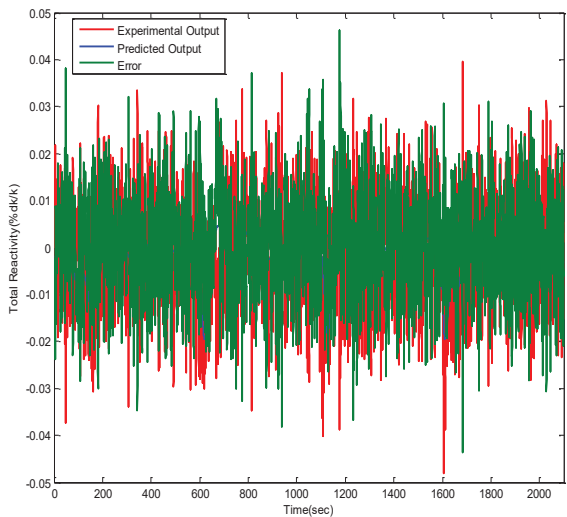


Fig. 12. Total reactivity of P-600 during validation phase of APD-ISO-DNS code.

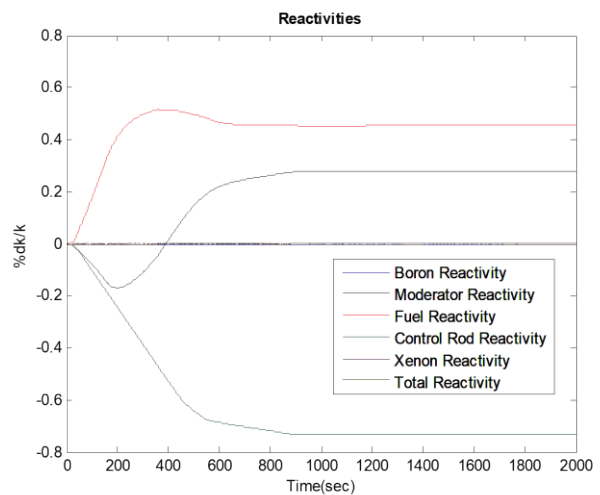


Fig. 13. Reactor dynamics of P-300 during validation phase of APD-ISO-DNS code..

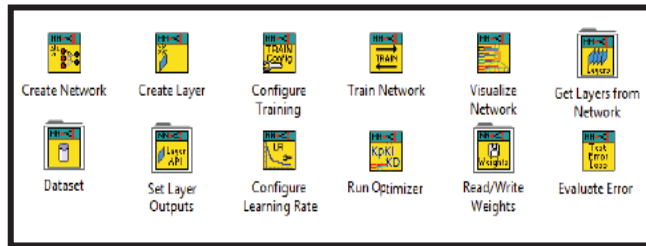


Fig. 14. PID optimizer based intelligent DANN VIs in APD-ISO-DNS LabVIEW code.

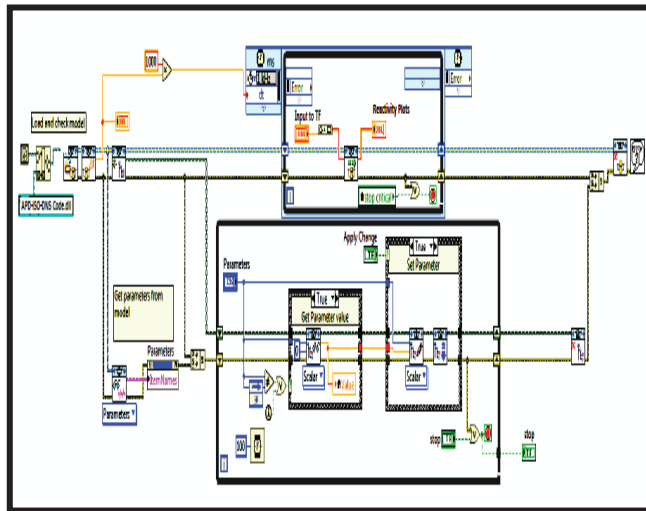


Fig. 15. Block Diagram of APD-ISO-DNS LabVIEW Code.

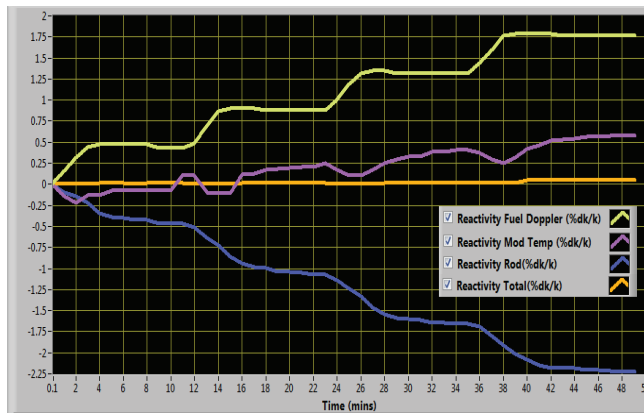


Fig. 16. Front Panel of Reactor dynamics of ACP-1000 during validation phase in APD-ISO-DNS Code.

#### 4. CONCLUSIONS

The reactor neutronics of three different generations of PWR based nuclear power plants have been considered in this research work. A state-of-the-art advanced multi-model PWR Dynamics and Intelligent Neutronics Simulation Code has been modeled, fine-tuned and simulated for P-300, AP-600 and ACP-1000 PWR based nuclear power plants. The developed computational transient analysis code for advanced multi-model PWR emerged as APD-ISO-DNS Code has three modules APD-ISO-DNS-300, APD-ISO-DNS-600 and APD-ISO-DNS-1000 which are evaluated under various load change transient conditions with different combinations of reactivity mechanisms in normal operation of PWR and reactor criticality is maintained and ensured as per benchmarks of Final Safety Analysis Reports (FSARs). Simulations have been conducted and performance of APD-ISO-DNS Code has been evaluated in a hybrid SIMULINK and LabVIEW environments and found optimal for future development of innovative advanced PWR nuclear power plant dynamics and accident analysis codes.

#### 5. ACKNOWLEDGEMENTS

The support of the Pakistan Atomic Energy Commission, Chashma Centre of Nuclear Training and Computer Development Division of KANUPP is gratefully acknowledged.

#### 6. REFERENCES

1. M. Subekti, S. Bakhri, and G. R. Sunaryo. The simulator development for RDE reactor. *Journal of Physics* 962: (2018).
2. M. Johnson, S. Lucas, and P. Tsvetkov. Modeling of reactor kinetics and dynamics. Idaho National Laboratory, Report Idaho Falls, Idaho 83415, U.S. Department of Energy, Canada (2010).
3. W. K. Lam. Advanced pressurized water reactor simulator. *IAEA Workshop on NPP Simulators for Education, Bucharest, Romania* (2006).
4. L. C. C. Po. PCTTRAN/PWR. Report Montville, New Jersey 07045, *IAEA Workshop on NPP Simulators for Education, Bucharest, Romania* (2006).
5. L. C. C. Po. PC-based simulator for education in advanced nuclear power plant construction. *International Symposium on the Peaceful Application of Nuclear Technology in the GCC Countries* (2008).
6. A. S. Mollah. Education tool for simulation of safety and transient analysis of a pressurized water reactor. *International Journal of Integrated Sciences & Technology* 03: 01-10 (2018).
7. S. M. A. Ibrahim. Thermal hydraulic simulations of a PWR nuclear power plant. *International Journal of Safety and Security* 013 (01): 31-520 (2019).
8. A. H. Malik, A. A. Memon, and M. R. Khan. Identification of nonlinear dynamics of nuclear power reactor using adaptive feedforward neural network. *Proceedings of Pakistan Academy Sciences* 47 (2): 111-120 (2010).
9. Z. Wenjie, Q. Jiang, Jinsen X. and T. Yu. A functional variable universe fuzzy PID controller for load following operation of PWR with the multiple model. *Annals of Nuclear Energy* 140: 1-6 (2020).
10. S. U. E. Hakim, A. Abimanyu, and Sutanto. Simulator design of Kartini reactor based on LabVIEW. *Journal forum Nukir* 12 (1): 29-41 (2018).
11. L. A. Macedo, W. M. Torres, G. Sabundjian, D. A. Andrade, A. B. Junior, P. E. Umbehaun, T. N. Conti, R. N. Mesquita, P. H. F. Masotti, and G. Angelo. Development of a LabVIEW web-based simulator for RELAP. *International Nuclear Atlantic Conference, Brazil*: 01-13 (2011).
12. J. Park, J. Jang, H. Kim, .Choe, D. Yun, and P. Zhang. RAST-K V2-Three-Dimensional nodal diffusion code for pressurized water reactor core analysis. *Energies* 13: 01-21 (2020).
13. X. Cui, W. Zhang, Z. Tuske, and M. Picheny. Evolutionary stochastic gradient descent for optimization of deep neural networks. *32 Conference on Neural Information Processing Systems, Canada*: (2018).
14. W. An, H. Wang, Q. Sun, J. Xu, Q. Dai, and L. Zhang. A PID controller approach for stochastic optimization of deep neural networks. *IEEE / CVF Conference on Computer Vision Pattern Recognition*: (2018).
15. H. Wang, Y. Luo, W. An, Q. Sun, J. Xu, and L. Zhang. PID controller-based stochastic optimization acceleration for deep neural networks. *IEEE Transactions on Neural Networks and Learning Systems* 31 (12): 1-10 (2020).
16. J. H. Horng. Hybrid MATLAB and LabVIEW with neural network to implement a SCADA system of AC servo motor. *Advances in Engineering Software* 39: 149-155 (2008).

